Penerbit Akademia Baru

Journal of Advanced Research in Micro and Nano Engineering

Journal homepage:
https://www.akademiabaru.com/submit/index.php/armne/index
ISSN: 2756-8210

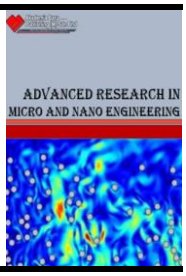

Comparative Analysis of $LiCo_{0.6}Sr_{0.4}O_2$ Cathode Electrochemical Performance in Oxide- and Proton-Conducting Intermediate-Temperature Solid Fuel Oxide Cells

Nur Nadhihah Mohd Tahir[1], Nurul Akidah Baharuddin[1,*], Mahendra Rao Somalu[1], Andanastuti Muchtar[1,2], Abdullah Abd Samat[3], Lai Jian Wei[4]

[1] Solid Oxide Fuel Cell Group, Fuel Cell Institute, Universiti Kebangsaan Malaysia, UKM, Bangi, Selangor 43600, Malaysia
[2] Department of Mechanical and Manufacturing Engineering, Faculty of Engineering and Built Environment, Universiti Kebangsaan Malaysia, Bangi, Malaysia
[3] Faculty of Mechanical Engineering and Technology, Universiti Malaysia Perlis (UniMAP), Pauh Putra Campus, 02600 Arau, Perlis, Malaysia
[4] Orbiting Scientific & Technology Sdn. Bhd, 35-1 Jalan Radin Anum 1, Bandar Baru Seri Petaling, Kuala Lumpur 57000, Malaysia

ARTICLE INFO

Article history:
Received 29 September 2023
Received in revised form 1 November 2023
Accepted 10 December 2023
Available online 31 January 2024

Keywords:
Solid oxide fuel cell; lithium; cathode; oxide-conducting; proton-conducting

ABSTRACT

Solid fuel oxide cells (SOFCs) are made up of three main parts: anode, electrolyte, and cathode. The main challenge in SOFCs is their high operating temperature, which can reach 1000 °C and lead to cell degradation issues. To address this, the utilization of lithium-based materials is suggested for the cathode component, facilitating intermediate-temperature SOFC operation within the temperature range of 500 to 800 °C. Previous studies have demonstrated the potential of producing high-quality lithium-based cathode ink using a triple-roll mill (TRM). By employing the fabrication parameters recommended in these studies, the lithium-based cathode, $LiCo_{0.6}Sr_{0.4}O_2$ (LCSO) was tested in different working environments, specifically the oxide-conducting SOFC (O^{2-} – SOFC) and proton-conducting SOFC (H^+ – SOFC). The LCSO inks were screen-printed on $Sm_{0.2}Ce_{0.8}O_{1.9}$ (for O^{2-} – SOFC) and $BaCe_{0.54}Zr_{0.36}Y_{0.1}O_{2.95}$ (for H^+ – SOFC) electrolyte before the analysis. Electrochemical impedance spectroscopy (EIS) and scanning electron microscopy (SEM) are used to characterize the electrochemical performance and morphology of the LCSO cathode. Based on the results, the LCSO cathode is found to respond well in O^{2-} – SOFC environment with an area-specific resistance (ASR) value of 0.75 Ωcm^2 compared to H^+ – SOFC which shows an ASR value higher by 11.45 Ωcm^2.

1. Introduction

For the past decade, lithium-based materials have been introduced by researchers due to their effectiveness in maintaining electrochemical performance of SOFCs at moderate-low operating temperatures [1]. Earlier researchers reported that with the presence of these lithium-based materials, oxygen concentration can be improved to a greater level, especially at grain boundaries.

* *Corresponding author.*
E-mail address: akidah@ukm.edu.my

https://doi.org/10.37934/armne.15.1.2230

Consequently, ionic conductivity can also be enhanced [2]. After selecting a highly promising cathode material that exhibits good electrochemical performance, the quality of the cathode layer or component also needs to be considered.

To achieve good electrochemical performance, the quality of the cathode layer needs improvement and refinement in order to produce a smooth and high-quality coating. This is because having high-quality coating facilitates the production of uniform cathode layers more easily. Various methods are employed by researchers to produce high-quality cathode coatings, including manual mixing, ball milling, and triple-roller milling (TRM) methods [3-5]. The cathode ink produced using the TRM method is known to be capable of providing a cathode film with a more homogeneous particle distribution [6,7].

Furthermore, our previous study has also identified the optimal parameters for utilizing a triple-roll mill in producing lithium-based cathode ink, specifically regarding roller speed and roller gap size [8,9]. Both studies conclude that certain parameters significantly impact the electrochemical performance in SOFC applications. The first study highlights that a gap size of 40 µm leads to the best results with the lowest area-specific resistance (ASR) of 4.16 Ωcm², showcasing the importance of high-quality lithium-based cathode [9]. The second study focuses on roller speed, revealing that the lowest ASR value of 16.17 Ωcm² is achieved at 300 rpm for LCSO ink [8]. This emphasizes the crucial role of processing technique in optimizing electrochemical performance.

Lithium-based cathode materials are recognized for their usability as electrodes in both oxide-conducting (O^{2-} – SOFC) and proton-conducting SOFC (H^{+} – SOFC) modes [10]. Given that our previous research predominantly concentr ated on enhancing the quality of cathode ink, the evaluation of the LSCO cathode's performance in these two environments remains unexplored. Therefore, the main objective of this study is to compare the electrochemical performance of the LCSO cathode in the settings of oxide-conducting and proton-conducting SOFCs.

2. Methodology

2.1 LCSO Cathode Powder Preparation

The cathode material LCSO, which is a modified new material, has been successfully produced in the SOFC laboratory, SELFUEL UKM, using a wet chemical process known as the glycine-nitrate combustion (GNC) method. To produce the cathode material, solutions and mixtures were prepared based on stoichiometric calculations following the ABO_3 perovskite structure. In this study, the perovskite structure is represented by A = Li, B = Co, Sr, and O = O. To generate the LCSO cathode powder, the necessary precursor chemicals or raw materials are strontium nitrate ($SrNO_3$), cobalt nitrate ($CoNO_3$), lithium nitrate ($LiNO_3$), and glycine (NH_2CH_2COOH) (Merck - Sigma-Aldrich). The composition of the raw materials is determined through stoichiometric calculations as shown in the Eq. (1) below

$$LiNO_3 + 0.6Co(NO_3)_2 + 0.4Sr(NO_3)_2 + yNH_2CH_2COOH \longrightarrow LiCo_{0.6}Sr_{0.4}O_{2-\delta} + AN_2 + BCO_2 + CH_2O \quad (1)$$

The total oxidation valence for the nitrate in this material is -15, while the total reduction valence for glycine $\Sigma_{glisina}$ is +9. Subsequently, the stoichiometric coefficient of the element ($ø_e$) will be calculated using Eq. (2) as shown below

($ø_e$) = total oxidation valence for the nitrate / -1 × total reduction valence for glycine (2)
(øe) = y = 1.7

Therefore, the nitrate molecules are calculated as follows

$$\sum(NO_3) = 1(NO_3) + [0.6\times2(NO_3)] + [0.4\times2(NO_3)] \quad (3)$$
$$\sum(NO_3) = 3$$

The stoichiometric ration for glycine to nitrate (G/N) can be calculated using Eq. (4)

$$(G/N)_s = (\phi_e) / \Sigma(NO_3) \quad (4)$$
$$(G/N)_s = 0.56$$

The value of (G/N) is utilized to calculate coefficients such as A, B, and C based on the chemical equilibrium principle

$$y = (\phi_e) = 1.7 \quad (5)$$

$$A = \Sigma(NO_3) + y] / 2 = (3+1.7)/2 = 2.35 \quad (6)$$

$$B = 2y = 2(1.7) = 3.4 \quad (7)$$

$$C = 5y/2 = 5/2(1.7) = 4.25 \quad (8)$$

All the coefficient values (A, B, and C) obtained will then be reintroduced into Eq. (1), resulting in the derivation of Eq. (9)

$$LiNO_3+0.6Co(NO_3)_2+0.4Sr(NO_3)_2+1.7NH_2CH_2COOH\rightarrow LiCo_{0.6}Sr_{0.4}O_{2-\delta}+2.35N_2+3.4CO_2+4.25H_2O \quad (9)$$

The weighed amounts of $Co(No_3)_2$, $Sr(NO_3)_2$ and $Li(NO_3)_2$, based on their respective stoichiometry, were dissolved in 100 mL of deionized water. The $Co(NO_3)_2$ solution was poured into a 1000 mL-sized beaker first (this beaker would be used in the combustion process), followed by the addition of $Sr(NO_3)_2$. The solution was then stirred using a magnetic stirrer for 10 minutes. Afterward, $Li(NO_3)_2$ was added to the solution and stirred for 30 minutes at room temperature. Once the materials were fully dissolved, glycine (NH_2CH_2COOH) was added to the solution and stirred for 18 hours [9-11].

Following this, the solution was stirred continuously while gradually raising the hotplate's temperature to reach a range of 250 °C to 300 °C, enabling the combustion of the materials and nitrates. Afterward, the resulting black ash precursor powder was additionally dried at 120 °C for 12 hours in a drying oven. The initial raw powder was then finely ground using an agate mortar to achieve a fine and smooth texture. Lastly, the dried, finely prepared precursor powder underwent calcination at 800 °C in a high-temperature furnace (Berkeley Scientific, USA) for a duration of 5 hours.

2.2 LCSO Ink Preparation

Calcined LCSO powders were then put through a ball milling process to disintegrate any agglomeration that may have grown while the calcination process was taking place. To ensure that the particle was properly disseminated, a dispersant of KD15 was used. After being milled for around 12 h in a container containing 200 ml of acetone, the mixture was then allowed to dry in an oven for a period of 5 h. After that, the remaining sediments from the powder were sieved for the next step

of the process. Following that, the powder was physically combined with a vehicle; a mixture of terpineol and ethyl cellulose. The preliminary mixed ink/slurry was then transferred to be processed by utilizing the TRM, and the roller speed and gap were adjusted accordingly. This ink or slurry was processed using TRM at a speed of 300 rpm and a gap size of 40 µm. Figure 1 shows the production of LCSO inks via TRM.

Fig. 1. Cathode inks production via triple-roll milling (TRM)

2.3 Symmetrical Cells Fabrication

The high-quality LCSO inks were then printed five times on both sides of the electrolyte. For O^{2-} – SOFC, cathode ink was printed on the cerium-doped samarium (SDC) electrolyte to construct an LCSO|SDC|LCSO symmetrical cell, while $BaCe_{0.54}Zr_{0.36}Y_{0.1}O_{2.95}$ (BCZY) is utilized as the electrolyte for H^{+} – SOFC to form a symmetrical cell with configuration of LCSO|BCZY|LCSO. The active area for both samples is maintained at 1 cm^2. The printed symmetrical cells were subsequently subjected to sintering at 800°C for 2 hours. Figure 2 shows the symmetrical cell for both configurations.

Fig. 2. Symmetrical cells for the electrochemical impedance spectroscopy analysis

2.4 Electrochemical Impedance Spectroscopy

Electrochemical impedance spectroscopy was conducted under a dry air atmosphere to assess the electrochemical performance of sintered symmetrical cells. The Autolab PGSTAT302N (Autolab 302, Eco Chemie, Netherlands), together with a frequency response analyzer in potentiostatic mode, was employed to determine the electrochemical impedance. This was carried out over a frequency range of 0.01 Hz to 1 MHz at an amplitude voltage of 20 mV and a temperature of 800 °C. To calculate the cathode's ASR, the obtained impedance spectra were transformed into Nyquist plots and analyzed using the NOVA 1.11 software.

3. Results

3.1 Electrochemical Impedance Spectroscopy Analysis

The ASR value is measured using the technique of electrochemical impedance spectroscopy (EIS) on symmetrical cells (cathode|electrolyte|cathode). EIS is also known as alternating current impedance spectroscopy using several parameters such as sinusoidal voltage values in the range of 5 – 20 mV and specific frequencies in the range of 100 mHz – 1 MHz [12]. The results from EIS can be used to determine the performance of chemical reactions occurring within a material system for specific components. The values of real impedance (Z_{real}) and imaginary impedance (Z_{imag}) can be obtained from EIS measurements. Data for both of these values at different frequencies are typically plotted as an impedance spectrum known as a Nyquist plot, as shown in Figure 3.

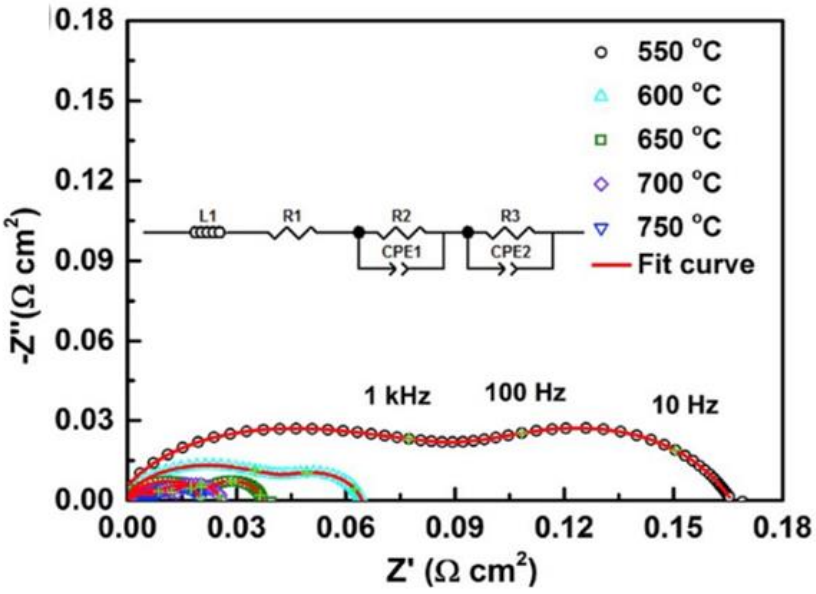

Fig. 3. Impedance spectrum (Nyquist plot) for symmetrical cell [13]

The ASR value is equivalent to the total polarization resistance, R_p, for the cathode component over a specific active surface area (A) [14]. All R_p values for the investigated cathodes are derived from the analysis of EIS. Eq. (10) represents the calculation formula for the cathode ASR value from the R_p values obtained through EIS analysis

$$ASR = (R_{p(total)} * A) / 2 \quad (10)$$

Figure 4 shows the Nyquist plot of EIS impedance spectra for the LCSO cathode ink in different SOFC environments, along with the employed equivalent circuit model used to analyze the impedance. As observed, there are two arcs, each representing the protonic environment, namely BCZY and SDC, which respectively symbolize the oxide-based SOFC environment. The cell was tested at 800 ℃ for both environments. In the O^{2-} – SOFC environment (SDC electrolyte), the ASR value measured 0.75 Ωcm², while in the H^{+} – SOFC environment (BCZY electrolyte), the recorded ASR value was 11.45 Ωcm². Referring to literature work [15], symmetrical cell of SOFCs are usually expected to have an ASR value between 0.1 and 1 Ωcm². In this work, ASR results for both types of SOFCs show that only the oxide-conducting SOFC meets this requirement with an ASR value of 0.75 Ωcm², which is within the acceptable range [16]. On the other hand, the proton-conducting SOFC doesn't meet this requirement, as its ASR value of 11.45 Ωcm² exceeds the acceptable range for symmetrical SOFCs (refer Table 1).

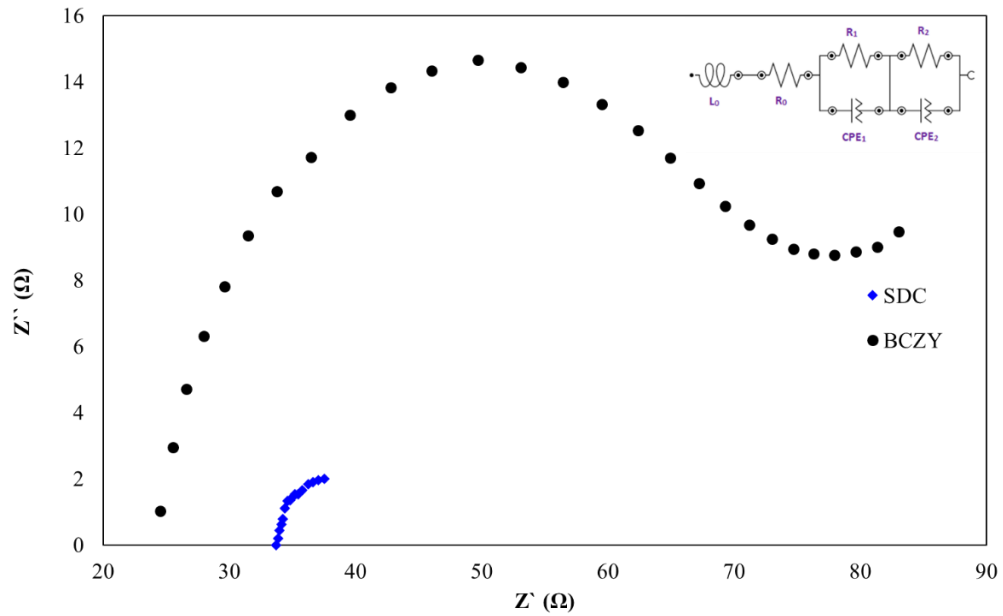

Fig. 4. Nyquist plot for the LCSO cathode tested under different environments (O^{2-} – SOFC with SDC electrolyte and H^{+} – SOFC with BCZY electrolyte) at 800 °C

Table 1
ASR-value comparison for LCSO cathode in different environments

ASR O^{2-} – SOFC	ASR H^{+} – SOFC
0.75 Ωcm²	11.45 Ωcm²

Additionally, the LCSO material shows a high thermal compatibility with the SDC electrolyte, as seen in the micrograph image in Figure 5, where the electrode and electrolyte layers adhere effectively [17-20].

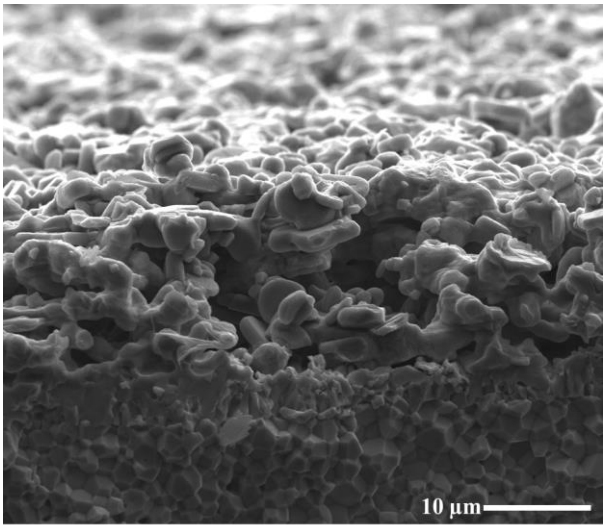

Fig. 5. FESEM cross-sectioned micrograph for LCSO|SDC after EIS test

4. Conclusions

As a conclusion, LCSO cathode in the conventional SOFC environment (O^{2-} – SOFC), exhibited the most favorable outcome with lower ASR values compared to the proton-conducting SOFC. Specifically, the ASR values were 0.75 Ωcm² and 11.45 Ωcm² respectively.

Acknowledgement

The authors acknowledge the Fundamental Research Grant Scheme (FRGS), grant No. FRGS/1/2021/TK0/UKM/01/5 funded by the Ministry of Higher Education (MOHE), Malaysia and Universiti Kebangsaan Malaysia for providing facilities and expertise that greatly assisted this research.

References

[1] Ramadhani, F., Mohd Azlan Hussain, Hazlie Mokhlis, and S. Hajimolana. "Optimization strategies for Solid Oxide Fuel Cell (SOFC) application: A literature survey." *Renewable and Sustainable Energy Reviews* 76 (2017): 460-484. https://doi.org/10.1016/j.rser.2017.03.052

[2] Jamil, Siti Munira, Mohd Hafiz Dzarfan Othman, Mukhlis A. Rahman, Juhana Jaafar, Mohamad Azuwa Mohamed, Mohd Zamri Mohd Yusop, Ahmad Fauzi Ismail, and Masaki Tanemura. "Dual-layer hollow fiber MT-SOFC using lithium doped CGO electrolyte fabricated via phase-inversion technique." *Solid State Ionics* 304 (2017): 113-125. https://doi.org/10.1016/j.ssi.2017.03.031

[3] Olowojoba, Ganiu, Shyam Sathyanarayana, Burak Caglar, Bernadeth Kiss-Pataki, Irma Mikonsaari, Christof Hübner, and Peter Elsner. "Influence of process parameters on the morphology, rheological and dielectric properties of three-roll-milled multiwalled carbon nanotube/epoxy suspensions." *Polymer* 54, no. 1 (2013): 188-198. https://doi.org/10.1016/j.polymer.2012.11.054

[4] Ratso, Sander, Andrea Zitolo, Maike Käärik, Maido Merisalu, Arvo Kikas, Vambola Kisand, Mihkel Rähn et al. "Non-precious metal cathodes for anion exchange membrane fuel cells from ball-milled iron and nitrogen doped carbide-derived carbons." *Renewable Energy* 167 (2021): 800-810. https://doi.org/10.1016/j.renene.2020.11.154

[5] Somalu, Mahendra R., Andanastuti Muchtar, Wan Ramli Wan Daud, and Nigel P. Brandon. "Screen-printing inks for the fabrication of solid oxide fuel cell films: A review." *Renewable and Sustainable Energy Reviews* 75 (2017): 426-439. https://doi.org/10.1016/j.rser.2016.11.008

[6] Abdul Samat, Abdullah, Mahendra Rao Somalu, Andanastuti Muchtar, Oskar Hasdinor Hassan, and Nafisah Osman. "LSC cathode prepared by polymeric complexation method for proton-conducting SOFC application." *Journal of Sol-Gel Science and Technology* 78 (2016): 382-393. https://doi.org/10.1007/s10971-015-3945-4

[7] Wan Yusoff, Wan Nor Anasuhah, Mahendra Rao Somalu, Nurul Akidah Baharuddin, Andanastuti Muchtar, and Lai Jian Wei. "Enhanced performance of lithiated cathode materials of LiCo0. 6X0. 4O2 (X= Mn, Sr, Zn) for proton-conducting solid oxide fuel cell applications." *International Journal of Energy Research* 44, no. 14 (2020): 11783-11793. https://doi.org/10.1002/er.5819

[8] Yusoff, Wan Nor Anasuhah Wan, Nur Nadhihah Mohd Tahir, Nurul Akidah Baharuddin, Mahendra Rao Somalu, Andanastuti Muchtar, and Lai Jian Wei. "Effects of roller speed on the structural and electrochemical properties of LiCo0. 6Sr0. 4O2 cathode for solid oxide fuel cell application." *Sustainable Energy Technologies and Assessments* 56 (2023): 103096. https://doi.org/10.1016/j.seta.2023.103096

[9] Tahir, N., N. Baharuddin, W. N. A. W. Yusoff, A. Aziz, M. Somalu, and Andanastuti Muchtar. "Physical and electrochem-ical characteristics of LiCo 0.6 Sr 0.4 O 2 cathode ink for intermediate-low temperature solid oxide fuel cell." *Malays. J. Anal. Sci* 26 (2022): 640-651.

[10] Tahir, Nur Nadhihah Mohd, Nurul Akidah Baharuddin, Abdullah Abdul Samat, Nafisah Osman, and Mahendra Rao Somalu. "A review on cathode materials for conventional and proton-conducting solid oxide fuel cells." *Journal of Alloys and Compounds* 894 (2022): 162458. https://doi.org/10.1016/j.jallcom.2021.162458

[11] Cui, Jinghao, Yuhan Gong, Runze Shao, Shaoshuai Wang, Jialun Mao, Meng Yang, Weifeng Wang, and Qingjun Zhou. "Electrode properties of a spinel family, AFe 2 O 4 (A= Co, Ni, Cu), as new cathode for solid oxide fuel cells." *Journal of Materials Science: Materials in Electronics* 30 (2019): 5573-5579. https://doi.org/10.1007/s10854-019-00851-x

[12] Nasani, Narendar, Devaraj Ramasamy, Ana D. Brandao, Aleksey A. Yaremchenko, and Duncan P. Fagg. "The impact of porosity, pH2 and pH2O on the polarisation resistance of Ni–BaZr0. 85Y0. 15O3− δ cermet anodes for Protonic Ceramic Fuel Cells (PCFCs)." *international journal of hydrogen energy* 39, no. 36 (2014): 21231-21241. https://doi.org/10.1016/j.ijhydene.2014.10.093

[13] Zhang, Wenwen, Lifang Zhang, Kai Guan, Xiong Zhang, Junling Meng, Haocong Wang, Xiaojuan Liu, and Jian Meng. "Effective promotion of oxygen reduction activity by rare earth doping in simple perovskite cathodes for intermediate-temperature solid oxide fuel cells." *Journal of Power Sources* 446 (2020): 227360. https://doi.org/10.1016/j.jpowsour.2019.227360

[14] Abd Aziz, Azreen Junaida, Nurul Akidah Baharuddin, Mahendra Rao Somalu, and Andanastuti Muchtar. "Review of composite cathodes for intermediate-temperature solid oxide fuel cell applications." *Ceramics International* 46, no. 15 (2020): 23314-23325. https://doi.org/10.1016/j.ceramint.2020.06.176

[15] Bernadet, Lucile, Carlos Moncasi, Marc Torrell, and Albert Tarancón. "High-performing electrolyte-supported symmetrical solid oxide electrolysis cells operating under steam electrolysis and co-electrolysis modes." *International Journal of Hydrogen Energy* 45, no. 28 (2020): 14208-14217. https://doi.org/10.1016/j.ijhydene.2020.03.144

[16] Yoo, Young-Sung, Yeon Namgung, Aman Bhardwaj, Sun-Ju Song, Young-Sung Yoo, Yeon Namgung, Aman Bhardwaj, and Sun-Ju Song. "A Facile Combustion Synthesis Route for Performance Enhancement of La 0.6 Sr 0.4 Co 0.2 Fe 0.8 O 3-δ (LSCF6428) as a Robust Cathode Material for IT-SOFC." *Journal of the Korean Ceramic Society* 56, no. 5 (2019): 497-505. https://doi.org/10.4191/kcers.2019.56.5.05

[17] Rahman, Hamimah Abd, Andanastuti Muchtar, Norhamidi Muhamad, and Huda Abdullah. "Structure and thermal properties of La0. 6Sr0. 4Co0. 2Fe0. 8O3− δ–SDC carbonate composite cathodes for intermediate-to low-temperature solid oxide fuel cells." *Ceramics International* 38, no. 2 (2012): 1571-1576. https://doi.org/10.1016/j.ceramint.2011.09.043

[18] Ullmann, H., N. Trofimenko, F. Tietz, D. Stöver, and A. Ahmad-Khanlou. "Correlation between thermal expansion and oxide ion transport in mixed conducting perovskite-type oxides for SOFC cathodes." *Solid state ionics* 138, no. 1-2 (2000): 79-90. https://doi.org/10.1016/S0167-2738(00)00770-0

[19] Zhou, Yu, Kouhei Takahashi, Swathi VR Naidu, Vipin Kumar, Tomohiro Yokozeki, Teruya Goto, and Tatsuhiro Takahashi. "Comparison of semi-doped PANI/DBSA complex achieved by thermal doping and roll-mill process: A new perspective for application." *Polymer* 202 (2020): 122723. https://doi.org/10.1016/j.polymer.2020.122723

[20] Hashim, Siti Salwa, Fengli Liang, Wei Zhou, and Jaka Sunarso. "Cobalt-free perovskite cathodes for solid oxide fuel cells." *ChemElectroChem* 6, no. 14 (2019): 3549-3569. https://doi.org/10.1002/celc.201900391